Far-infrared spectroscopic investigations on CuO

G. Kliche
Max-Planck-Institut für Festkörperforschung, Heisenbergstrasse 1, 7000 Suttgart 80, West Germany

Z. V. Popovic
Institute of Physics, P. O. Box 57, 11000 Belgrade, Yugoslavia

(Received 23 July 1990)

Far-infrared reflection spectra of a polycrystalline sample of monoclinic CuO were measured in the frequency range from 30 to 700 cm^{-1} at temperatures between 10 and 300 K. The six observed lattice vibrational modes at 147, 161, 321, 478, 533, and 587 cm^{-1} (300 K) were assigned by comparison with those of PdO using Cartesian symmetry coordinates. Normal coordinates were calculated within a short-range valence-force-field model. A broad mode at about 414 cm^{-1} at 300 K, whose intensity changes drastically as the temperature is lowered, may be explained in terms of magnetic ordering in CuO.

I. INTRODUCTION

Square planar CuO_2 layers play a decisive role in high-temperature superconductivity. Thus properties of CuO-based materials have been extensively investigated during the past several years. Although several coupling modes have been proposed, phonons and charge and spin fluctuations among others, there still is no common understanding of the pairing mechanisms leading to superconductivity. If we are to make headway, a grasp of the phonon behavior and a knowledge of the magnetic ordering of CuO-based materials is a prerequisite. An important tool for this purpose is the investigation of phonons and magnons in high-temperature superconductors with infrared and Raman spectroscopies.[1,2] The measurement of infrared-active optical-phonon frequencies in high-temperature superconductors is complicated by strong plasmon-phonon interaction in the conducting CuO_2 layers. In ceramic samples many phonon modes are hidden by the broad background of the collective free carrier contribution to the spectra. Therefore, an investigation of similar semiconducting compounds with low free carrier concentrations yields useful data on the interatomic potentials which may be transferred for mode assignment in the CuO-based superconductors. The infrared and Raman spectra of a series of ternary and quarternary compounds structurally related to the high-temperature superconductors were investigated recently[1,2] but, hitherto, the infrared spectrum of the binary copper (II) oxide, CuO, has remained unassigned.

Infrared spectra of CuO were measured by several authors. Most recently, Hagemann *et al.*[3] measured the infrared absorption spectrum of polycrystalline CuO, dispersed in paraffine oil, in the frequency range between 200 and 700 cm^{-1}. Hanuza *et al.*,[4] Popovic *et al.*,[5] and Degiorgi *et al.*[6] measured the fir-reflection spectra of CuO in order to evaluate CuO as a possible impurity phase in high-temperature superconducting oxides. The analysis of the vibrational spectrum of CuO may prove a most effective tool in the study of the Cu^{2+} and O^{2-} interactions. In this paper we present infrared reflection data obtained on a polycrystalline sample of CuO. Despite the fact that the primitive cell of CuO contains only two formula units, the infrared spectrum is complex and difficult to interpret. We were able to assign the observed modes by correlation with the spectrum of the structurally closely related but higher symmetric palladium oxide (PdO), and with the help of approximate normal coordinate calculations using a short-range valence force field model. An unusual temperature dependence of one of the observed modes is discussed in relation to the magnetic ordering in CuO.

II. CRYSTAL STRUCTURE AND FACTOR GROUP ANALYSIS

The semiconducting copper(II) oxide (CuO) crystallizes in the monoclinic space group $C2/c$-C_{2h}^6 (No. 15) with four formula units in the crystallographic unit cell.[7] The lattice constants are $a=4.6837$ Å, $b=3.4226$ Å, $c=5.1288$ Å, $\beta=99.54°$. The positions of the atoms are Cu $(4c)$:1:$(\frac{1}{4},\frac{1}{4},0)$,2:$(\frac{3}{4},\frac{1}{4},\frac{1}{2})$,O$(4e)$:3:$(0,y,\frac{1}{4})$,4:$(0,\bar{y},\frac{3}{4})$, $y=0.4184$; the equivalent positions are (0,0,0) and $(\frac{1}{2},\frac{1}{2},0)$. Copper forms four coplanar bonds with oxygen, which itself is coordinated by four copper atoms in a distorted tetrahedral environment. The whole three-dimensional network of the CuO crystal structure is built from two sets of chains $^1_\infty[CuO_{4/2}]$ directed along [110] and $[1\bar{1}0]$ and staggered along [001], Fig. 1. Factor group analysis using the tables given by Rousseau *et al.*[8] yields

$$\mathrm{Cu}(C_i):\ \Gamma=3A_u+3B_u\ ,$$

$$\mathrm{O}(C_2):\ \Gamma=A_g+2B_g+A_u+2B_u\ ,$$

$$\Gamma_{\mathrm{CuO}}^{\mathrm{tot}}=A_g+2B_g+4A_u+5B_u\ .$$

Of these, $1A_u(T_y)$ and $2B_u(T_x,T_z)$ are acoustical modes, so that the total of vibrational modes ($\mathbf{q}=0$) and their activity is

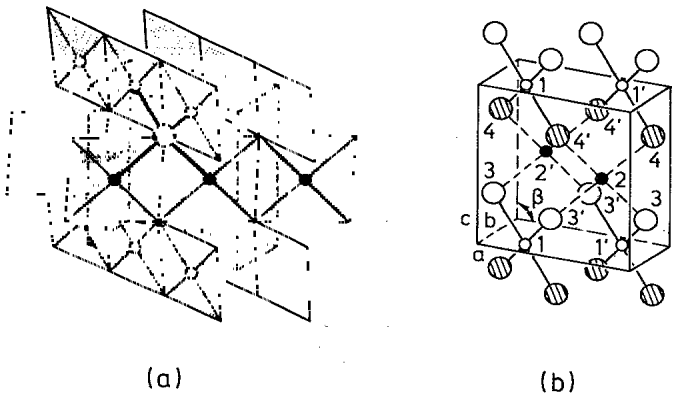

FIG. 1. The crystal structure of CuO ($C2/c-C_{2h}^6$, $Z=4$). (a) Staggering of chains $^1_\infty[CuO_{4/2}]$, the tetrahedral coordination of oxygen is indicated. (b) Crystallographic unit cell of CuO. Atoms 1,2: copper (small circles); 3,4: oxygen (large circles). The Cartesian symmetry coordinates, derived using the projection operator technique (Ref. 18), are A_g:$S_1=y_3-y_4$; B_g:$S_2=x_3-x_4$, $S_3=z_3-z_4$; A_u:$S_4=x_1-x_2$, $S_5=y_1+y_2$, $S_6=z_1-z_2$, $S_7=y_3+y_4$; B_u:$S_8=x_1+x_2$, $S_9=y_1-y_2$, $S_{10}=z_1+z_2$, $S_{11}=x_3+x_4$, $S_{12}=z_3+z_4$.

$$\Gamma_{CuO}^{vib}=A_g(R)+2B_g(R)+3A_u(\text{ir})+3B_u(\text{ir})\ . \qquad (1)$$

Thus, three Raman-(A_g,B_g) and six infrared-(A_u,B_u) active modes are to be expected in the spectra of CuO. (In the usual character tables of point group C_{2h} the c axis is special and therefore T_z transforms as A_u. To describe the lattice vibrations of monoclinic CuO the common crystallographic set up with b as the special axis was used in the present work. Thus, T_y transforms as A_u.)

III. SAMPLE PREPARATION, FAR-INFRARED AND RAMAN SPECTRA

Polycrystalline samples of CuO were prepared by oxidation of high-purity copper powder in air at 700 °C. The samples were checked by x-ray-diffraction methods. Pressed pellets of the obtained polycrystalline CuO were used for the measurement of the fir-reflection spectra (Bruker IFS 113v, Oxford model CF 100 cryostat). Pellets pressed at room temperature yield a maximum Reststrahlen reflectivity of about 30% at 300 K.[5] From hot pressed and polished pellets (graphite die, 600 °C, subsequent annealing at 700 °C in air and pellet checking by x-ray powder diffraction) a maximum reflectivity of about 50% was reached. The spectra obtained from cold and hot pressed samples differ somewhat because of different orientations of the crystallites, but the main features are the same. The fir-reflection spectra of hot pressed CuO at 300, 200, 160, and 10 K are shown in Fig. 2. At room temperature, two sharp low-frequency modes at 147 and 161 cm^{-1}, one less intense mode at 321 cm^{-1}, and a broad and complex feature between 340 and 630 cm^{-1}, with maxima at 414, 478, 533, and a shoulder at 587 cm^{-1}, may be observed. Although the measurements were performed on polycrystalline samples, and furthermore, the polarization direction of pure TO-LO phonon modes is given from symmetry only for the A_u modes

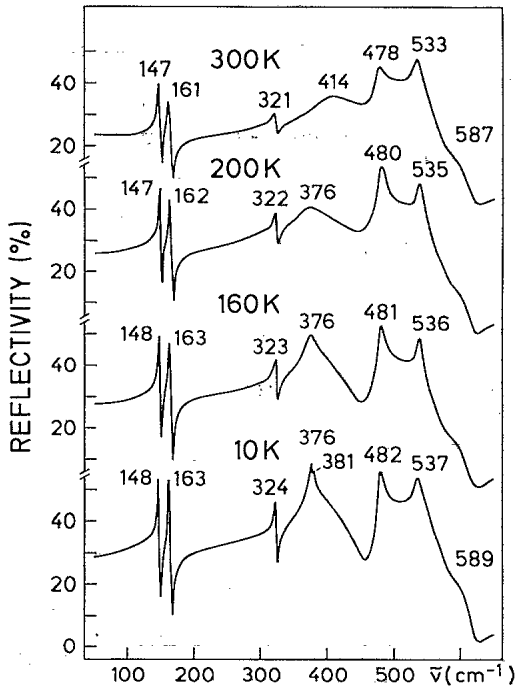

FIG. 2. Far-infrared reflection spectra (Bruker IFS 113v) of a hot pressed pellet of polycrystalline CuO at 300, 200, 160, and 10 K.

whereas the B_u TO-LO modes depend on the special macroscopic field in the (101) plane,[9] we analyzed the spectra by means of a Kramers-Kronig transformation. The quasi-TO-LO phonon frequencies of the three sharp low-frequency modes, determined in the conventional manner from the maxima of the $\mathrm{Im}(\hat{\epsilon})$ and $-\mathrm{Im}(1/\hat{\epsilon})$ functions, are 147-150, 161-166, and 321-323 cm^{-1} (at 300 K). The dielectric function peaks are not clearly resolved for the high-frequency modes. It may be concluded qualitatively from the broad and mutually overlapping bands that the ionicity of CuO is high despite the strong covalent bonds which are indicated by the square planar coordination of copper. With decreasing temperature the modes at 147, 161, 321, 478, 533, and 587 cm^{-1} (300 K) sharpen and slightly increase in frequency to 148, 163, 324, 482, 537, and 589 cm^{-1} at 10 K, respectively. This was to be expected from the anharmonicity of the lattice vibrations. More striking is the fact that below 200 K, i.e., below the Néel temperature of 230 K of antiferromagnetic CuO,[10] the frequency of the broad mode at 414 cm^{-1} shifts to 376 cm^{-1}. On further cooling the frequency of this mode is rather constant, but its intensity increases and it becomes the strongest mode at 10 K. Additional splitting (376, 381 cm^{-1}) and a shoulder on the high-frequency tail of this mode are observed at low temperatures. Our results (300 K) are basically in agreement with known reflection spectra.[5,6] The only difference is in an increase of the reflectivity at low frequencies in the spectrum given in Ref. 6, which is not observed in our sample and may be due to metallic impurities or surface defects of the sample measured by these authors.

The Raman spectrum of CuO was recently investigated

by several authors on both polycrystalline samples and single crystals. For our hot pressed sample we found phonon peaks at 301, 348, and 633 cm^{-1}.[11] This is in good agreement with the result obtained by Hagemann *et al.*[3] for CuO single crystals. From this and other investigations[12,13] the assignment of the modes is clearly 296 (301) cm^{-1}: A_g; 344 (348) cm^{-1}: B_g^1; 629 (633) cm^{-1}: B_g^2.

IV. ASSIGNMENT OF THE VIBRATIONAL MODES

An assignment of the vibrational modes of CuO can be performed by comparison with those of PdO.[14] The crystal structure of CuO is a distorted version of the tetragonal PdO structure.[15] The two crystal structures are compared in Fig. 3. In the projection along [001] it is seen that the two chains $^1_\infty[MO_{4/2}]$ (M = Pd,Cu) intersect at an angle of 90° in PdO and ≈75° in CuO. The primitive cell of the C-centered CuO structure [defined by the vectors $\mathbf{a}_1$, $\mathbf{b}_1$ (Fig. 3), $\mathbf{c}_1 \equiv c$] corresponds to the primitive tetragonal unit cell of PdO (space group $P4_2/mmc - D^9_{4h}$); it contains two CuO formula units. The C_2 axis of the C_{2h} factor group of CuO correlates to the C_2'' axis of the D_{4h} factor group of PdO as indicated in Fig. 3. Thus, the correlation $D_{4h} \rightarrow C_{2h}$ is[16] $B_{1g} \rightarrow B_g$; $E_g \rightarrow A_g + B_g$; $A_{2u} \rightarrow B_u$; $B_{2u} \rightarrow A_u$; $E_u \rightarrow A_u + B_u$. The representation of the lattice vibrations of PdO is[14]

$$\Gamma^{\text{tot}}_{\text{PdO}} = 2A_{2u}(\text{ir}, T_z) + 3E_u(\text{ir}, T_x, T_y) + B_{2u}(s) + B_{1g}(R) + E_g(R) .$$

The correlation for CuO yields

$$\Gamma^{\text{tot}}_{\text{CuO}} = 5B_u + 4A_u + 2B_g + A_g ,$$

in agreement with the factor-group analysis result [Eq. (1)].

In the infrared spectrum of PdO, a low frequency out-of-plane bending mode of E_u symmetry is observed at 160 cm^{-1}. This mode should split into $A_u^1 + B_u^1$ in CuO. The two bands at 147 and 161 cm^{-1} in the reflection spectrum of CuO are assigned to these modes. In the out-of-plane bending mode of an MX_4 planar square unit the central atom M moves perpendicularly to the plane. In CuO this movement is similar but the eigenvector decomposes along the x and y directions and bond stretching forces become important. Since the $^1_\infty[CuO_{4/2}]$ chains intersect the x axis at $\alpha' \approx 37°$ and the y axis at $\beta' \approx 53°$ (Fig. 3), to first order one finds an anisotropy splitting due to the bond stretching contribution of

$$\frac{\tilde{\nu}_x}{\tilde{\nu}_y} = \left[\frac{\cos 37}{\cos 53}\right]^{1/2} = 1.15 . \quad (2)$$

The A_u out-of-plane symmetry coordinate is $x_1 - x_2$, the corresponding B_u coordinate being $y_1 - y_2$ (see caption of Fig. 1). Thus one can expect the A_u mode at higher frequency. The $\tilde{\nu}(A_u)/\tilde{\nu}(B_u) = \frac{161}{147} = 1.12$ ratio is in good agreement with the assumed anisotropy splitting.

The same argument holds for the difference between the low-frequency Raman active modes A_g and B_g^1, correlating to E_g in PdO (not observed in Ref. 14). Only oxygen atoms are involved in the Raman active modes, the symmetry coordinates being A_g: $y_3 - y_4$, B_g^1: $x_3 - x_4$. Thus, $A_g < B_g^1$ is to be expected, as is in accordance with the experiment (A_g:301,B_g^1:348 cm^{-1}). The B_g^2 mode (633 cm^{-1}) of CuO corresponds to the B_{1g} (652 cm^{-1}) of PdO. The B_g^1 and B_g^2 frequencies are well separated in CuO. Mixing of the two modes is negligible and the B_g^2 normal coordinate is thus approximately the symmetry coordinate $z_3 - z_4$.

Let us now return to the discussion of the infrared

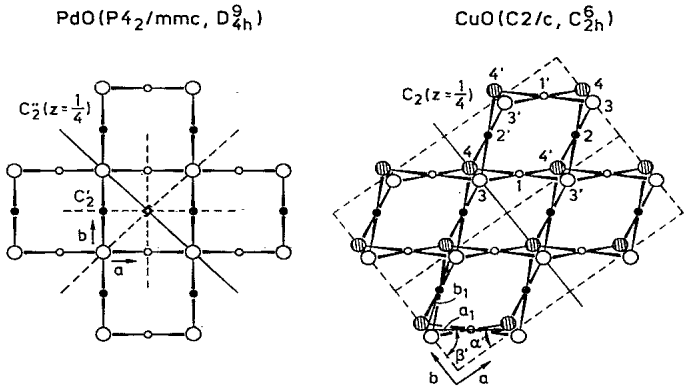

FIG. 3. Projection of the crystal structures of PdO ($P4_2/mmc - D^9_{4h}$) and CuO ($C2/c - C^6_{2h}$) along [001]. Small circles: Pd (Cu), large circles: O. The C_2'' axis $(x,x,\frac{1}{4})$ in $P4_2/mmc$ (PdO) corresponds to the C_2 axis $(0,y,\frac{1}{4})$ in $C2/c$ (CuO). $\mathbf{a}_1, \mathbf{b}_1$ are the base vectors of the CuO primitive cell which intersect the crystallographic axes a and b with $\alpha' \approx 37°$, $\beta' \approx 53°$.

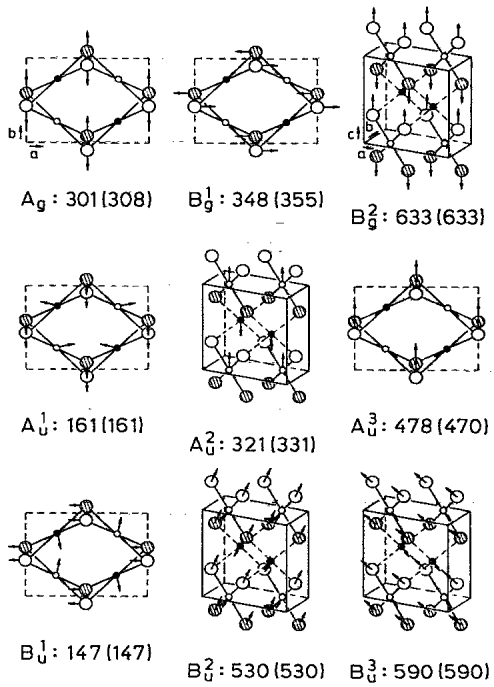

FIG. 4. q=0 normal mode displacements of copper oxide (CuO). Experimental (calculated) phononfrequencies are given.

spectrum. Obviously, the low-intensity mode at 321 cm^{-1} in the infrared spectrum of CuO is the A_u^2 mode z_1-z_2, corresponding to the B_{2u} silent mode in PdO (B_{2u}^{calc}:242 cm^{-1}). The assignment of the broad modes in the high-frequency range is difficult and in principle not accurate from the powder data. The large TO-LO splitting and the monoclinic crystal structure of CuO are the main cause of the complex spectral features. From the correlation with PdO one is led to expect the remaining A_u^3, B_u^2, and B_u^3 stretching modes in this range. At the highest frequency in the infrared spectrum of CuO we expect the B_u^3 vibration $(z_1+z_2)-(z_3+z_4)$, correlating with the A_{2u} mode of PdO. The shoulder at 587 cm^{-1} is assigned to this mode. In terms of the symmetry coordinates the E_u mode of PdO splits into $(y_1+y_2)-(y_3+y_4)$(A_u^3) and $(x_1+x_2)-(x_3+x_4)$ (B_u^2). Furthermore, the anisotropy splitting discussed above predicts $A_u^3<B_u^2$ and we assign the modes at 478 and 533 cm^{-1} to these modes, respectively. Their ratio is 1.12, in good agreement with Eq. (2). The result of our assignment is summarized in Table II ($\tilde{\nu}_{expt}$). The vibrational frequencies obtained from the reflection spectrum of polycrystalline CuO lie somewhere between the TO and LO phonon modes. Only the highest determined LO has to correspond exactly to the LO (B_u^3). Single crystal investigation is needed for the accurate determination of the frequencies.

It may be seen in Fig. 2 that the temperature dependence of the 414-cm^{-1} mode differs totally from that of the others. We thus conjecture that the origin of this mode is not an $q=0$ infrared-active optical-phonon as will be discussed later.

V. NORMAL COORDINATE ANALYSIS

In order to confirm the qualitative assignment given above, a normal coordinate calculation was performed. Because of the uncertainties in the experimentally obtained frequencies the calculation can be approximate only. Wilson's GF-matrix method[17] was applied in a version similar[18] to that extended by Shimanouchi *et al.*[19] for the calculation of the optically active ($q=0$) lattice vibration frequencies. Only short-range forces were considered.

The coordinations of the atoms in the crystal structure of monoclinic CuO are complex. A large number of internal coordinates must be included in a lattice dynamical calculation. To reduce the number of parameters the force constants f'_{jk} were related to the interatomic distances r'_{jk} using

$$f'_{jk}=f^0_{jk}\left[\frac{r^0_{jk}}{r'_{jk}}\right]^n. \tag{3}$$

This formula was used by Maroni *et al.*[20] for the calculation of the vibrational modes of $La_{2-x}M_xCuO_4$ (M =Sr,Ba). They found $n=6$, which we used in our approximate calculation also.

We successively considered the Cu-O (1.95–4.09 Å, calc. 1), O-O (2.62–3.92 Å, calc. 2), and Cu-Cu (3.08–3.74 Å, calc. 3) interactions and fitted the three independent force constants f^0_{jk} to the experimental frequencies. The interactions between the nonbonded O-O, Cu-Cu, and Cu-O (third and higher order neighbors) partly represent the O-Cu-O, Cu-O-Cu bending and the $[CuO_{4/2}]$ out-of-plane bending coordinates which are not explicitly considered in the calculations, therefore. In calc. 1, only involving the copper-oxygen bond stretching interactions (1.95–4.09 Å), a value of $f^0_{Cu\text{-}O}$ (1.95 Å)=1.37 mdyn $Å^{-1}$ fits the A_u^3, B_u^2, and B_u^3 frequencies. The sequence of all calculated frequencies agrees with that predicted by the Cartesian symmetry coordinates, i.e., $A_g<B_g^1<B_g^2, B_u^1<A_u^1, A_u^2<A_u^3<B_u^2<B_u^3$. Calculation 2 includes the oxygen-oxygen interaction (2.62–3.92 Å) as well, the force constants obtained are $f^0_{Cu\text{-}O}=1.37$, $f^0_{O\text{-}O}$ (2.62 Å)=0.28 mdyn $Å^{-1}$. This shifts the B_g^2 mode

TABLE I. Experimental ($\tilde{\nu}_{expt}$) and calculated ($\tilde{\nu}_{calc}$) phonon frequencies (cm^{-1}), interatomic distances (r,Å), force constants (f, mdyn $Å^{-1}$), and potential energy distribution (%) of CuO (calc. 4, see text). Force constants resulting in P.E.D. values <10% are omitted.

	r	f	A_g	B_g^1	B_g^2	A_u^1	A_u^2	A_u^3	B_u^1	B_u^2	B_u^3
$\tilde{\nu}_{expt}$[a]			301	348	633	161	321	478	147	530	590
$\tilde{\nu}_{calc}$			308	355	633	161	331	470	147	530	590
Cu-O	1.95	1.28	97	72	22	1	4	70	1	78	7
	1.96	1.24	24	77	35	5	52	14	0	15	76
	2.78	0.15	23	4	1	44	1	7	47	3	0
	3.41	0.04	7	1	0	9	0	3	10	0	0
O-O	2.62	0.27	5	0	27	0	0	0	0	0	0
Cu-Cu	3.08	0.11	0	0	0	1	15	0	32	0	0
	3.17	0.09	0	0	0	23	2	1	0	0	0
$f^i_{1,1}$[b]	180.0	−0.18	−14	−10	−3	0	0	10	0	11	1
$f^i_{1,2}$	84.3	0.27	−21	−32	12	1	−7	13	0	−15	10
$f^i_{1,2}$	95.7	0.32	−24	−38	14	−1	8	−15	0	17	−12
$f^i_{1,2}$	104.0	0.21	−16	25	−9	0	5	−10	0	−11	8
$f^i_{2,2}$	180.0	−0.19	−3	−11	−5	1	8	2	0	2	11

[a] A_u^1, A_u^2,B_u^1: Reststrahlen maxima, A_u^3,B_u^2,B_u^3 approximate frequencies were used in the calculations.
[b] Interaction terms $f^i_{j,k}$ between the internal coordinates. $j,k=1$: Cu-O, 1.95 Å; $j,k=2$: Cu-O, 1.96 Å. The angle between j and k is given in the second column.

TABLE II. Mass-adjusted L_{XSM} eigenvectors (Ref. 19) of CuO, calc. 4 (see text). The Cartesian symmetry coordinates S_i are defined in the caption of Fig. 1. The A_g normal coordinate is identical S_1.

	B_g^1	B_g^2		A_u^1	A_u^2	A_u^3		B_u^1	B_u^2	B_u^3
$\tilde{\nu}_{calc}$	355	633	$\tilde{\nu}_{calc}$	161	331	470	$\tilde{\nu}_{calc}$	147	530	590
S_2	0.99	0.02	S_4	0.90	−0.21	0.39	S_8	0.13	−0.20	0.38
S_3	−0.02	0.99	S_5	0.19	0.04	−0.41	S_9	0.95	0.21	−0.23
			S_6	0.15	0.97	0.19	S_{10}	0.03	−0.39	−0.22
			S_7	−0.37	−0.10	0.81	S_{11}	−0.27	0.40	−0.75
							S_{12}	−0.06	0.77	0.44

to the right. The high value of the B_g^2 frequency is due to oxygen-oxygen repulsion, see Fig. 4. The interaction between the copper atoms is introduced in calc. 3, yielding $f^0_{Cu\text{-}O}=1.37$, $f^0_{O\text{-}O}=0.28$, $f^0_{Cu\text{-}Cu}$ (3.08 Å)$=0.10$ mdyn Å^{-1}. This improves the fit of A_u^1, A_u^2, and B_u^1 and the overall agreement becomes satisfactory, with the exception of the A_g and B_g^1 modes. The experimental frequencies of the latter are considerably lower than those calculated. Therefore, in calc. 4 interaction terms between connected Cu-O bonds (1.95 Å, 1.96 Å) were introduced. Physically, these terms represent the fact that the vibrations of the interconnected $[CuO_{4/2}]$ are strongly coupled and many-body interactions are involved. This coupling is especially strong for the A_g and B_g^1 modes, consisting of mutual compression and depression of Cu-O bonds in the two chains. A rationalized treatment of the interaction terms was not performed, however. The individual terms contribute quite differently to the A_g, B_g, A_u, and B_u symmetry force constants and were used only as fitting parameters to adjust the frequencies.

Similar to Ohwada,[21] who studied the valence force field of La_2CuO_4, negative values for the trans-Cu-O–Cu-O interaction terms were found. This last fitting procedure seems to be rather arbitrary. But it was found that the main force constants $f_{Cu\text{-}O}$, $f_{O\text{-}O}$, $f_{Cu\text{-}Cu}$ and the vibrational eigenvectors, which also depend on the relative masses of the vibrating atoms, are only slightly different for calcs. 3 and 4 except the more strongly coupled B_u^2 and B_u^3 modes. The final fit gives good agreement between all experimental and calculated phonon frequencies and the results are summarized in Table I ($\tilde{\nu}_{expt}$,$\tilde{\nu}_{calc}$, force constants, and distribution of the potential energy) and Table II (mass adjusted L_{XSM}-eigenvectors[19]). Normal mode displacement patterns as obtained from Table II are shown in Fig. 4. The only deviation from the qualitative assignment using the Cartesian symmetry coordinates is that the B_u^2 and B_u^3 modes are strongly coupled. The highest frequency B_u^3 mode is a Cu-O stretching along $[\bar{1}01]$, B_u^2 the corresponding stretching along [101]. This is reasonable as the bond angles between the Cu-O-Cu chains are 145.8 and 108.8° for $[\bar{1}01]$ and [101], respectively. Obviously, the sum of the Cu-O–Cu-O interaction terms is more efficient along $[\bar{1}01]$.

VI. LOW-TEMPERATURE SPECTRA

Finally, we discuss the broad mode between 380 and 414 cm^{-1}. As has been noted, the intensity of this mode increases dramatically upon cooling (Figs. 2 and 5). The appearance of this mode and its anomalous temperature dependence may be explained in terms of antiferromagnetic ordering in CuO. Namely, the results of magnetic specific heat[22] measurements and neutron diffraction experiments[23,24] indicate a magnetic ordering at $T_N=230$ K first into a noncommensurable spiral structure, and then at $T_T=213$ K there is a transition to an antiferromagnetic phase consisting of ferromagnetic $(\bar{1}01)$ double planes with antiferromagnetic ordering along the $[\bar{1}01]$ direction. The integral intensity of the 414-cm^{-1} mode as a function of temperature is given in Fig. 6. At extrapolation the curve in Fig. 6 yields a value of 213 K, the temperature of antiferromagnetic ordering in CuO. In view of the fact that the temperature dependence of this mode is similar to that of the CuO Raman mode at 240 cm^{-1} (Ref. 12) which is due to magnetic excitation, i.e., to the temperature dependence of the magnetic susceptibility,[23] we conclude that the ir 414-cm^{-1} mode is due to antiferromagnetic ordering in CuO.

Magnetic ordering related ir absorption and reflection by semiconductors and dielectrics has not been as thoroughly investigated as Raman scattering.[25,26] The focus has been on magnetic-polariton modes.[27,28] It has been shown that ir active magnons usually occur at very low frequencies (below 100 cm^{-1}) and that ir magnon absorption does not change the reflectivity by more than 10%. Neutron spectroscopy indicates for CuO an optical magnon (for Γ point) at 187 cm^{-1}.[24] Published CuO Raman spectra[3,12,13] and the ir spectra shown in Fig. 2 indicate no magnon mode at this frequency. This low-intensity magnon mode may be masked by the 147- and 161-cm^{-1} phonons.

As we could not detect the $\mathbf{q}=0$ optical magnon, it is

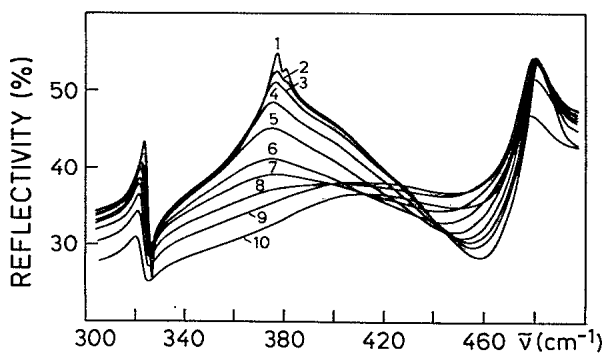

FIG. 5. Far-infrared reflection spectrum of CuO at different temperatures in an expanded scale. 1-10: 10, 120, 140, 160, 180, 200, 210, 225, 250, 300 K, respectively.

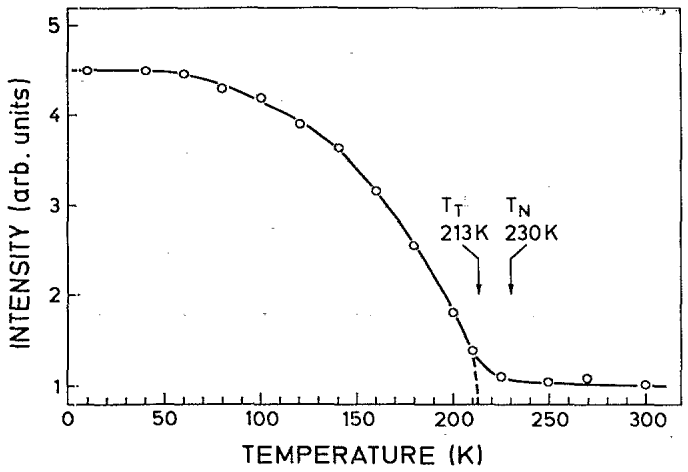

FIG. 6. Integral intensity of the 414-cm^{-1} mode of CuO as a function of temperature. The mode intensities are calculated from the reflectivity data between the phonon dips near 320 and 460 cm^{-1} (see Fig. 5), respectively, and normalized to the intensity determined at 300 K. The solid line is just a guide to the eye.

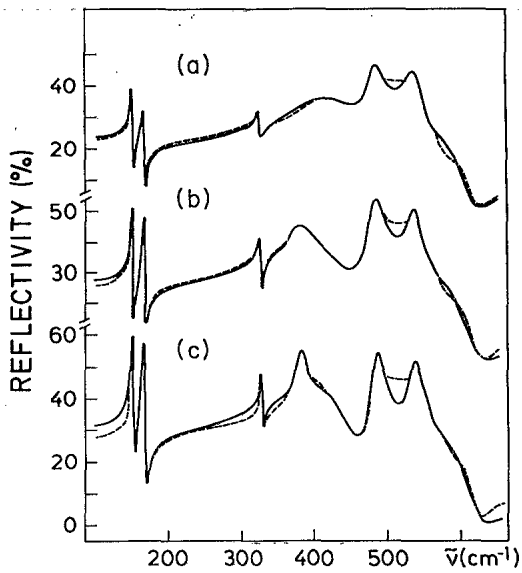

FIG. 7. Modeling the far-infrared reflection spectra of CuO at (a) 300, (b) 180, and (c) 10 K using the factorized form of the dielectric function (see text). Solid: calculated, dashed line: experimental reflectivity. The oscillator parameters are given in Table III.

hard to believe that the 414-cm^{-1} mode is due to $\mathbf{q}\neq 0$ magnons because they have to be weaker than the $\mathbf{q}=0$ magnon except if the magnon density of states is the highest at these frequencies. In view of the CuO magnon dispersion curves,[24] this is not the case.

It is worth noting that this mode is somewhat weaker than the surrounding phonon modes at room temperature, whereas at lower temperature it becomes stronger than them. This kind of magnetic interaction with infrared radiation in CuO is unique because magnetic Reststrahlen bands, as has been mentioned earlier, are usually weak.[28] With this in mind we conclude that the 414-cm^{-1} mode is a zone-boundary phonon mode which becomes infrared active due to the zone-folding effects induced by infrared absorption from antiferromagnetic superstructure.[29,30] Namely, the magnetic unit cell of CuO along the *a* and *c* axes is doubled with respect to the crystallographic unit cell. Thus, the CuO magnetic unit cell contains 4 formula units resulting in 24 phonon branches. Hence, new $\mathbf{q}=0$ optical modes appear as a result of the corresponding folding of the phonon branches. The phonon mode frequencies were determined using a fitting procedure based on

$$\hat{\epsilon}=\epsilon_\infty \prod_j \frac{\omega_{\mathrm{LO},j}^2-\omega^2-i\omega\gamma_{\mathrm{LO},j}}{\omega_{\mathrm{TO},j}^2-\omega^2-i\omega\gamma_{\mathrm{TO},j}}, \tag{4}$$

where $\omega_{\mathrm{TO},j}(\omega_{\mathrm{LO},j})$ and $\gamma_{\mathrm{TO},j}(\gamma_{\mathrm{LO},j})$ are transverse (longitudinal) frequencies and damping factors of mode j, respectively, and ϵ_∞ is the high-frequency dielectric constant. The application of Eq. (4) yields the results depicted in Figs. 7(a)–7(c). The dashed lines are the experimental reflectivity spectra, the full lines are calculated spectra obtained using the values listed in Table III.

At room temperature [Fig. 7(a)] in addition to the 6

TABLE III. Optical parameters (cm^{-1}) of phonons obtained by oscillator fitting of the CuO reflection spectra.

		300 K	180 K	10 K			300 K	180 K	10 K			300 K	180 K	10 K
1	ω_{TO}	147	147	147.5	4	ω_{TO}	479.5	478.5	479	7	ω_{TO}	410	378	379
	γ_{TO}	2	1.5	2		γ_{TO}	18	15	11		γ_{TO}	86	33	9.5
	ω_{LO}	150.5	151	152		ω_{LO}	480	479	480		ω_{LO}	430	379	380.5
	γ_{LO}	1	1.5	2		γ_{LO}	38	55	125		γ_{LO}	175	50	18
2	ω_{TO}	162.5	163.5	162.5	5	ω_{TO}	535	532	532	8	ω_{TO}		382	382
	γ_{TO}	5	3	2.5		γ_{TO}	27	23	20		γ_{TO}		100	100
	ω_{LO}	167.5	169	168.5		ω_{LO}	544	540	540		ω_{LO}		445	474
	γ_{LO}	3	3.5	3		γ_{LO}	30	35	35		γ_{LO}		150	45
3	ω_{TO}	321	323.5	325	6	ω_{TO}	587	587	587		ϵ_∞	6	6.2	6.2
	γ_{TO}	4.5	2	2		γ_{TO}	150	150	150					
	ω_{LO}	324	326.5	328		ω_{LO}	615	620	620					
	γ_{LO}	5	1.8	2		γ_{LO}	39	49	39					

phonon $q=0$ modes at 147, 162.5, 321, 479.5, 535, and 587 cm^{-1} a good fit was obtained with the introduction of an additional phonon mode at 410 cm^{-1}. The existence of this mode, however, is unusual above Néel's temperature, i.e., in the paramagnetic phase. This may be explained in terms of magnetic fluctuations at temperatures considerably above T_N, as confirmed by CuO neutron spectroscopy at room temperature.[24] As the correlation length of these magnetic fluctuations equals 60 Å at 300 K, zone-folding effects have to be present in the paramagnetic phase at room temperature, also. The intensity of this mode remains constant at cooling until T_N is reached (see Fig. 6). A good fit of the lower temperature spectra ($T < T_N$) requires two zone boundary phonon modes (Table IV). The appearance of a number of zone boundary phonons in the CuO infrared spectra is possible due to acoustic and optical phonon branch folding. The CuO magnetic group selection rules have to be concurrently satisfied. An additional difficulty in the determination of the CuO magnetic group is the disagreement on CuO spin orientation. In Ref. 23 the spins are found to be oriented along the b axes, whereas recent work[22] indicates that they are oriented along the a axis.

After the completion of the work presented here, a study of inelastic neutron scattering and lattice dynamics of CuO[31] came to our attention. These results confirm the infrared and Raman mode assignment presented in Sec. IV above and support our assumption on the existence of zone-folded modes in the infrared spectrum of CuO. Namely, at the X point of the CuO Brillouin zone two optical branches at about 12 THz appear to merge. This frequency corresponds to zone-boundary modes in Fig. 2 at 376 cm^{-1} and 381 cm^{-1}. Furthermore, the CuO magnetic excitation-related 240-cm^{-1} Raman mode[12] is probably a zone boundary mode which according to Ref. 31 appears at the X point of the CuO Brillouin zone at a frequency of 7.2 THz.

More information on CuO magnetic excitation will be forthcoming following infrared and Raman experiments on single crystalline samples with polarized light as well as with deeper insight into the phonon dispersion curves of this compound. This work is in progress.

ACKNOWLEDGMENTS

The authors thank W. König for the measurement of the fir spectra, Dr. M. Ain for sending the CuO lattice-dynamics results prior to publication, and Professor M. Cardona for helpful discussions.

[1]C. Thomsen and M. Cardona, in *Physical Properties of High Temperature Superconductors I*, edited by D. M. Ginsberg (World Scientific, Singapore, 1989), p. 409.
[2]R. Feile, Physica C **159**, 1 (1989).
[3]H. Hagemann, H. Bill, W. Sadowski, E. Walker, and M. Francois, Solid State Commun. **73**, 447 (1990).
[4]J. Hanuza, J. Klamut, R. Horyn, and B. Jezowska-Trzebiatowska, J. Mol. Struct. **193**, 57 (1989).
[5]Z. V. Popovic, C. Thomsen, M. Cardona, R. Liu, G. Stanisic, R. Kremer, and W. König, Solid State Commun. **66**, 965 (1988).
[6]L. Degiorgi, E. Kaldis, and P. Wachter, Physica C **153-155**, 657 (1988).
[7]S. Åsbrink and L. J. Norrby, Acta Crystallogr. Sec. B **26**, 8 (1970).
[8]D. L. Rousseau, R. P. Bauman, and S. P. S. Porto, J. Raman Spectrosc. **10**, 253 (1981).
[9]R. Claus, L. Merten, and J. Brandmüller, *Light Scattering by Phonon-Polaritons* (Springer, Berlin-Heidelberg, 1975).
[10]M. O'Keefe and F. S. Stone, J. Phys. Chem. Solids **23**, 261 (1962).
[11]The authors thank E. T. Heyen for the measurement of the Raman spectrum.
[12]J. C. Irwin, J. Chrzanowsky, T. Wei, D. J. Lockwood, and A. Wold, Physica C **166**, 486 (1990).
[13]J. Chrzanowski and J. C. Irwin, Solid State Commun. **70**, 11 (1989).
[14]G. Kliche, Z. Naturforsch. A **44**, 169 (1989).
[15]A. F. Wells, *Structural Inorganic Chemistry* (Clarendon, Oxford, 1984).
[16]W. G. Fateley, F. R. Dollish, N. T. McDevitt, and F. F. Bentley, *Infrared and Raman Selection Rules for Molecular and Lattice Vibrations: The Correlation Method* (Wiley, New York, 1972).
[17]E. B. Wilson, J. C. Decius, and P. C. Cross, *Molecular Vibrations, The Theory of Infrared and Raman Vibrational Spectra* (McGraw-Hill, New York, 1955).
[18]G. Kliche (unpublished).
[19]T. Shimanouchi and M. Tsuboi, J. Chem. Phys. **35**, 1597 (1961).
[20]V. A. Maroni, T. O. Brun, M. Grimsditch, and C.-K. Loong, Phys. Rev. B **39**, 4127 (1989).
[21]K. Ohwada, Spectrochim. Acta A **45**, 1137 (1989).
[22]E. Gmelin, U. Köbler, W. Brill, T. Chattopadhyay, and S. Sastry (unpublished).
[23]J. B. Forsyth, P. J. Brown, and B. M. Wanklyn, J. Phys. C **21**, 2917 (1988).
[24]M. Ain, W. Reichardt, B. Hennion, G. Pepy, and B. M. Wanklyn, Physica C **162-164**, 1279 (1989).
[25]N. Suzuki and H. Kamimura, J. Phys. Soc. Jpn. **35**, 985 (1973).
[26]M. Balkanski, M. Jouanne, G. Ouvrard, and M. Scagliotti, J. Phys. C **20**, 4397 (1987).
[27]D. L. Mills and E. Burstein, Rep. Prog. Phys. **37**, 817 (1974).
[28]K. M. Häussler, A. Lehmeyer, and L. Merten, Phys. Status Solidi B **111**, 513 (1982).
[29]B. X. Yang, T. R. Thurston, J. M. Tranquada, and G. Shirane, Phys. Rev. B **39**, 4343 (1989).
[30]G. Güntherodt and R. Zeyher, in *Topics in Applied Physics*, edited by M. Cardona and G. Güntherodt (Springer, Berlin-Heidelberg, 1984) Vol. 54.
[31]W. Reichardt, F. Gompf, M. Ain, and B. M. Wanklyn (unpublished).